Research Square

Preprints are preliminary reports that have not undergone peer review.
They should not be considered conclusive, used to inform clinical practice,
or referenced by the media as validated information.

Possibility of hypoxanthine oxidation mediated by mouse aldehyde oxidase in vivo

Kazuki Terada
Teikyo University
Tamaki Watanabe
Teikyo University
Nobuhiro Yasuno
Teikyo University
Makoto Hosoyamada
hosoyamada.makoto.pl@teikyo-u.ac.jp
Teikyo University

Article

Keywords: Aldehyde oxidase, N 1-methyl-2-pyridone-5-carboxamide, xanthine dehydrogenase gene knockout mice

Posted Date: June 18th, 2026

DOI: https://doi.org/10.21203/rs.3.rs-9288396/v1

License: This work is licensed under a Creative Commons Attribution 4.0 International License.
Read Full License

Additional Declarations: Competing interest reported. N.Y. declares to be the sponsored chair of lifetime education for pharmacist by AIN holdings Inc. Other authors declare no conflict of interest.

Version of Record: A version of this preprint was published at Scientific Reports on November 10th, 2026. See the published version at https://doi.org/10.1038/s41598-026-79081-1.

Abstract

Type 1 xanthinuria is characterized by elevated levels of xanthine in blood and urine but near absent amounts of uric acid. In humans, xanthine oxidoreductase (XOR) gene (*XDH*) mutations in type 1 xanthinuria do not affect lifespan whereas *Xdh* knockout (*Xdh*KO) mice die young. High activity allele of hypoxanthine phosphoribosyl transferase (Hprt(high))-*Xdh*KO-*Slc23a4* knockout (*Slc23a4*KO) mice survive to adulthood but exhibit renal damage with a low urinary hypoxanthine/xanthine ratio. Aldehyde oxidase (AOX), a homolog of XOR, is encoded by four genes in mice compared to a single gene in humans. If mouse AOX oxidizes hypoxanthine to xanthine, it could contribute to the observed species differences. Here, DBA/2 background *Xdh*KO mice with low AOX activity were generated, which exhibit reduced urinary N^1-methyl-2-pyridone-5-carboxamide (2-Py) excretion and increased urinary hypoxanthine/xanthine ratios.

Male C57BL/6 background Hprt(high)-*Xdh*KO-*Slc23a4*KO mice were mated with female DBA/2 mice to obtain 48 DBA/2 background *Xdh*KO mice. Urine samples were analyzed. In 16 *Xdh*KO-*Slc23a4*KO mice, distribution of the urinary 2-Py/Cr ratio versus the hypoxanthine/xanthine ratio showed an inverse correlation indicating AOX oxidizes hypoxanthine to xanthine.

Future work will involve disrupting *Aox2*, *Aox3*, and *Aox4*, leaving only *Aox1* functional in a Hprt(high)-*Xdh*KO-*Slc23a4*KO background to establish a mouse model for human xanthinuria type 1.

Introduction

Xanthine oxidoreductase (XOR) catalyzes the sequential conversion of hypoxanthine to xanthine and then to uric acid. Mutations in the human xanthine oxidoreductase gene (*XDH*) that abolish XOR activity result in type I xanthinuria, which is a rare autosomal recessive disorder characterized by elevated levels of xanthine in the blood and urine but correspondingly low or absent levels of uric acid. Human type I xanthinuria is considered a benign disease because although patients with this disorder suffer from urolithiasis, they typically live a normal life span. By contrast, mice lacking the *Xdh* gene (*Xdh*KO), which might be thought to model human type I xanthinuria, invariably die by 8 weeks of age.[1] This profound discrepancy in survival indicates that fundamental species differences exist in purine metabolism between humans and mice.

We previously generated Hprt(high)-*Xdh*KO-*Slc23a4*KO mice by replacing hypoxanthine phosphoribosyl transferase (HPRT) with a high-activity human allele and targeting of *Slc23a4*, a pseudogene in humans. These mice exhibited extended survival, and for the first time, adult *Xdh*KO mice were obtained. However, renal impairment persisted, and although offspring were delivered, they invariably died within one day after birth. Thus, further refinement was required to establish an accurate mouse model of human type I xanthinuria.[2]

In Hprt(high)-*Xdh*KO-*Slc23a4*KO mice, the urinary hypoxanthine/xanthine ratio (mol/mol) was lower than that observed in healthy patients with type I xanthinuria, resembling the findings in patients with renal

impairment. This result suggests that enhanced conversion of hypoxanthine to xanthine may underlie the renal dysfunction observed in these mice.[2] Aldehyde oxidase (AOX), a homolog of XOR, is encoded by a single gene (*AOX1*) in humans, whereas mice possess four homologs (*Aox1–Aox4*).[3] If mouse AOX2–AOX4 oxidize hypoxanthine to xanthine, AOX could contribute to the evident species differences in purine metabolism between humans and mice.

The aim of this study was to determine whether urinary excretion of N^1-methyl-2-pyridone-5-carboxamide (2-Py), a metabolite of N^1-methyl-nicotinamide reflecting AOX activity,[4,5] correlates with changes in the urinary hypoxanthine/xanthine ratio. To address this issue, we used DBA/2 mice (a low AOX activity strain) crossed with C57BL/6-Hprt(high)-Xdh KO-Slc23a4 KO mice (a high AOX activity strain).[4]

Materials and Methods

Male Hprt(high)-*Xdh*KO-*Slc23a4*KO mice on a C57BL/6 background were crossed with female DBA/2 mice (Japan CLEA, Tokyo, Japan), producing 48 DBA/2 background *Xdh*KO mice. Genotyping was performed according to previously published protocols.[2] In total, 289 mice from the breeding process were monitored. Spot urine samples (30 µL) were collected individually from each mouse in a plastic container.

All animal experiments and the experimental protocols were approved by the animal ethics committee of Teikyo University (Teikyo Animal Ethics #21 – 007). All methods were carried out in accordance with relevant guidelines and regulations.

Urinary metabolites were analyzed using high-performance liquid chromatography (HPLC) (Chromaster; Hitachi, Tokyo, Japan). Separation was achieved on a Unison US-C18 column (250 × 2.0 mm i.d., 5 µm particle size; Imtakt, Kyoto, Japan). The column temperature was maintained at 25°C, and the mobile phase consisted of 10 mM ammonium formate in water, delivered at a flow rate of 0.200 mL/min. Detection was performed at 234 nm for creatinine, hypoxanthine, and xanthine, and at 260 nm for 2-Py. Urine samples (2 µL) were diluted with 100 µL of the mobile phase prior to injection.

Statistical analysis was performed using regression analysis within the Analysis Tools of Microsoft® Excel® 2024.

All data generated or analysed during this study are included in this published article and its supplementary information files.

Results

The retention times for creatinine (Cr), N^1-methyl-4-pyridone-5-carboxamide (4-Py) and 2-Py were 5.700 min, 7.340 min and 26.007 min, respectively. In our analytical system, 2-Py was clearly detectable in mouse urine, whereas 4-Py was either undetectable or observed in only trace amounts. Therefore, the urinary 2-Py/Cr ratio (mol/mol) was used as an indicator of AOX activity in this study (Suppl. Figure 1).

In 289 DBA/2-C57BL/6 hybrid mice, the histogram of urinary 2-Py/Cr ratios (Fig. 1A) showed that the most frequent values were within the 0.020–0.025 range, with a minor peak observed at 0.055–0.060. The urinary 2-Py/Cr ratio of three DBA/2 strain mice was 0.035 ± 0.011 (mean ± SD, n = 3), which closely coincided with the most frequent peak. The urinary 2-Py/Cr ratio of four C57BL/6 strain mice was 0.102 ± 0.008 (mean ± SD). Samples with a urinary 2-Py/Cr ratio exceeding mean + 2SD (0.118) were considered outliers.

Of the 289 mice, 48 were *Xdh*KO mice. Outliers were examined for the hypoxanthine (HX)/Cr ratio, xanthine (XA)/Cr ratio, HX/XA ratio, XA/HX ratio, and (HX + XA)/Cr ratio in the urine of *Xdh*KO mice using Tukey's fences. As shown in the box plots (Fig. 1B), a total of 8 samples were identified as outliers: one mouse with the same XA/Cr ratio and (HX + XA)/Cr ratio, four mice with the HX/XA ratio, and three mice with the XA/HX ratio. Figure 1C shows the distribution of the 2-Py/Cr ratio - HX/XA ratio, with the 8 outliers marked with an "X" and three samples with a "+" mark indicating an outlier in the 2-Py/Cr ratio.

Figure 2A shows the distribution of the 2-Py/Cr ratio - HX/XA ratio in the urine of the remaining 37 *Xdh*KO mice after exclusion of the outliers. The regression equation was y = -1.23315x + 0.202485 (R^2 = 0.130912, p = 0.027768), showing an inverse correlation where the urinary HX/XA ratio significantly increased with decreasing urinary 2-Py excretion. As shown in Fig. 2B, the urinary (HX + XA)/Cr ratio was 3.754 ± 1.307 (mean ± SD) in *Xdh*KO-*Slc23a4*(-/-) mice (indicated by black circles) and 5.279 ± 1.617 (mean ± SD) in *Xdh*KO-*Slc23a4*(+/) mice (indicated by white circles), which are statistically significant differences (p = 0.004). The distributions of the urinary 2-Py/Cr ratio- HX/Cr ratio, XA/Cr ratio, XA/HX ratio are shown in Suppl. Figure 3A-3C, respectively.

Of the 37 *Xdh*KO mice, 16 were *Xdh*KO-*Slc23a4*KO mice. The distribution of the urinary 2-Py/Cr ratio - HX/XA ratio for these 16 mice is shown in Fig. 3A. The regression equation was y = -2.1032x + 0.251614 (R^2 = 0.329304, p = 0.020105), and a similar inverse correlation was evident, with the urinary HX/XA ratio significantly increasing with decreasing urinary 2-Py excretion. Furthermore, the regression equation for the distribution of the urinary 2-Py/Cr ratio and the XA/HX ratio, shown in Fig. 3B (y = 177.6625x + 3.632371, (R^2 = 0.270974, p = 0.038707)), confirmed a correlation between a decrease in urinary 2-Py excretion and a significant decrease in the urinary XA/HX ratio.

In addition, the regression equation for the distribution of the urinary 2-Py/Cr ratio and the HX/Cr ratio in *Xdh*KO-*Slc23a4*KO mice, shown in Fig. 3C (y = -6.79345x + 0.78426, (R^2 = 0.369211, p = 0.012535)), displayed an inverse correlation between a decrease in urinary 2-Py excretion and a significant increase in the urinary HX/Cr ratio. The regression equation for the distribution of the urinary 2-Py/Cr ratio - XA/Cr ratio in *Xdh*KO-*Slc23a4*KO mice, shown in Fig. 3D, is y = 5.231622x + 3.044114 (r^2 = 0.01508, p = 0.650496). Although not statistically significant, this relationship suggests that a 1 molar decrease in hypoxanthine is associated with an approximately 0.77 molar increase in xanthine. The distribution of the urinary 2-Py/Cr ratio - (HX + XA)/Cr ratio is shown in Suppl. Figure 3a.

Discussion

Previous studies have demonstrated that *Aox* gene expression varies among mouse strains, with DBA/2 mice showing reduced expression of AOX1, AOX3 (formerly AOH1), and AOX4 (formerly AOH2) compared with the C57BL/6 strain.[4] Mouse AOX2 (formerly AOH3) is expressed only in the nasal mucosa and does not exhibit strain-dependent differences.[5] Reflecting these strain differences, urinary 2-Py excretion also varies among mouse strains, with DBA/2 mice showing lower urinary 2-Py excretion compared to B6 mice. [6]

In the present study, the distribution of the urinary 2-Py/Cr ratio was bimodal, likely reflecting the genetic contribution of high 2-Py-excreting C57BL/6 mice and low 2-Py-excreting DBA/2 mice from the parental lines. The peak corresponding to the urinary 2-Py/Cr ratio of 0.102 ± 0.008 (mean ± SD) in four C57BL/6 strain mice was absent, suggesting that lower urinary 2-Py excretion may be a dominant trait. The smaller peak observed in the 0.055–0.060 interval of the urinary 2-Py/Cr ratio likely represents mice with genetic backgrounds derived from both DBA/2 and C57BL/6 strains.

Regression analysis is susceptible to outliers, requiring appropriate outlier handling. Using Tukey's fences, a non-parametric method for identifying outliers in a dataset, we identified four samples as outliers in the HX/XA ratio and three samples as outliers in the XA/HX ratio. This processing effectively excluded the outliers prominently displayed in Fig. 1C and Suppl. Figure 2C, respectively.

SNBT1, the gene product of *Slc23a4*, is thought to be a transporter involved in the intestinal absorption of purine bases.[7] This study demonstrated that in *Xdh*KO mice, SNBT1 deficiency significantly reduced total purine excretion from 5.279 ± 1.617 to 3.754 ± 1.307. Therefore, inhibiting intestinal absorption of purine bases reduces urinary oxypurine excretion. However, the urinary (HX + XA)/Cr ratio, which indicates urinary total oxypurine excretion, remained largely unchanged with the decrease in 2-Py/Cr (Fig. 3E). Thus, it is possible that pseudogenization of *Aox* genes does not lead to a decrease in urinary total oxypurine excretion, but a decrease in urinary excretion of xanthine, because xanthine displays low water-solubility, a buildup of this metabolite could cause renal damage.

Although the inverse correlation between urinary 2-Py excretion and the urinary HX/XA ratio was significant ($p = 0.020105$), the R^2 ($R^2 = 0.329304$) was relatively weak. Indeed, *in vitro* experiments showed that N^1-methylnicotinamide metabolism primarily reflects the activity of AOX3 and AOX2,[8] whereas the expression of AOX1 and AOX4 is also reduced in DBA/2 mice. Therefore, if AOX1 or AOX4 contributes to hypoxanthine oxidation, urinary 2-Py excretion reflecting AOX3 and AOX2 activity may not strongly correlate with the hypoxanthine/xanthine ratio.

Whether hypoxanthine serves as a substrate for AOX has been investigated *in vitro* using isolated and expressed mouse *Aox1–4* genes.[8] The results suggested that hypoxanthine was not a substrate for mouse AOX1–4. However, AOX purified from rabbit liver converted hypoxanthine to xanthine, although not to uric acid.[9] Based on these findings, it can be hypothesized that AOX2–AOX4, which are expressed only in mice, may similarly convert hypoxanthine to xanthine *in vivo*. In support of this, the present study observed an inverse correlation between urinary 2-Py excretion and the urinary hypoxanthine/xanthine

ratio, suggesting that AOX catalyzes the conversion of hypoxanthine to xanthine in mice. The lack of activity observed *in vitro* may be attributable to suboptimal reaction conditions or the requirement for cofactors. For example, oxidation of the hypoxanthine analog allopurinol by purified rat AOX was performed at pH 9.0.[10] Optimizing reaction conditions is expected to be extremely difficult. Thus, it may not be possible to conclusively demonstrate that mouse AOX2-4 oxidizes hypoxanthine to xanthine in an *in vitro* experimental system. However, we believe research into pseudogenes that mimic the three *Aox*3, *Aox*4, and *Aox*2 genes *in vivo*, similar to those found in humans, warrants further investigation.

Conclusion

This study provides the first evidence that mouse AOX may participate in the oxidation of hypoxanthine to xanthine using *Xdh*KO mice. These findings provide new insights beyond previous *in vitro* studies, suggesting that mouse AOX can oxidize hypoxanthine *in vivo*. Future work will involve genome editing to disrupt *Aox*2, *Aox*3, and *Aox*4, leaving only *Aox*1 functional on a Hprt(high)-*Xdh*KO-*Slc23a4*KO background. We anticipate this approach will establish a mouse model that closely mimics human xanthinuria type 1.

Declarations

Conflict of Interest

N.Y. declares to be the sponsored chair of lifetime education for pharmacist by AIN holdings Inc. Other authors declare no conflict of interest.

Competing Interests

N.Y. declares to be the sponsored chair of lifetime education for pharmacist by AIN holdings Inc. Other authors declare no conflict of interest.

Author Contribution

K. T. contributed draft of the work; T. W. and N. Y. contributed substantively revised it. M.H. contributed all of this study.

Data Availability

All data generated or analyzed during this study are included in this published article and its supplementary information files.

Research funding

This study was partly supported by Grants-in Aid for Scientific Research from Japan Society for the Promotion of Science (to M. H., Grant Number: No. 26460347, No. 17K08605 and No. 22K08320)

References

1. Ohtsubo, T., Rovira, I. I., Starost, M. F., Liu, C. & Finkel, T. Xanthine oxidoreductase is an endogenous regulator of cyclooxygenase-2. *Circ. Res.* **95**, 1118–1124 (2004).
2. Terada, K. et al. Pseudogenization of the Slc23a4 gene is necessary for the survival of Xdh-deficient mice. *Sci. Rep.* **15**, 3250 (2025).
3. Terao, M., Garattini, E., Romao, M. J. & Leimkuhler, S. Evolution, expression, and substrate specificities of aldehyde oxidase enzymes in eukaryotes. *J. Biol. Chem.* **295**, 5377–5389 (2020).
4. Vila, R. et al. Regulation and biochemistry of mouse molybdo-flavoenzymes. The DBA/2 mouse is selectively deficient in the expression of aldehyde oxidase homologues 1 and 2 and represents a unique source for the purification and characterization of aldehyde oxidase. *J. Biol. Chem.* **279**, 8668–8683 (2004).
5. Kurosaki, M. et al. The aldehyde oxidase gene cluster in mice and rats. Aldehyde oxidase homologue 3, a novel member of the molybdo-flavoenzyme family with selective expression in the olfactory mucosa. *J. Biol. Chem.* **279**, 50482–50498 (2004).
6. Maeta, A., Sano, M., Fukuwatari, T. & Shibata, K. Simultaneous measurement of nicotinamide and its catabolites, nicotinamide N-oxide, N(1)-methyl-2-pyridone-5-carboxamide, and N(1)-methyl-4-pyridone-3-carboxamide, in mice urine. *Biosci. Biotechnol. Biochem.* **78**, 1306–1309 (2014).
7. Yamamoto, S. et al. Identification and functional characterization of the first nucleobase transporter in mammals: implication in the species difference in the intestinal absorption mechanism of nucleobases and their analogs between higher primates and other mammals. *J. Biol. Chem.* **285**, 6522–6531 (2010).
8. Kucukgoze, G. & Leimkuhler, S. Direct comparison of the four aldehyde oxidase enzymes present in mouse gives insight into their substrate specificities. *PLoS One*. **13**, e0191819 (2018).
9. Krenitsky, T. A., Neil, S. M., Elion, G. B. & Hitchings, G. H. A comparison of the specificities of xanthine oxidase and aldehyde oxidase. *Arch. Biochem. Biophys.* **150**, 585–599 (1972).
10. Moriwaki, Y. et al. In vitro oxidation of pyrazinamide and allopurinol by rat liver aldehyde oxidase. *Biochem. Pharmacol.* **46**, 975–981 (1993).

Figures

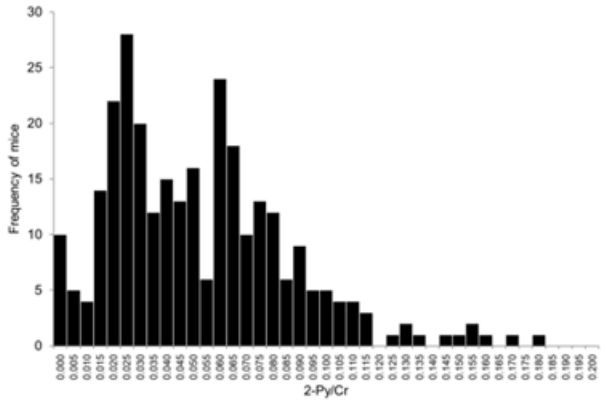


Figure 1A. Histogram of frequency of mice divided into classes of urinary 2-Py/Cr
The distribution of frequency of mice by grouping it into classes of the 0.005 width of urinary 2-Py/Cr.

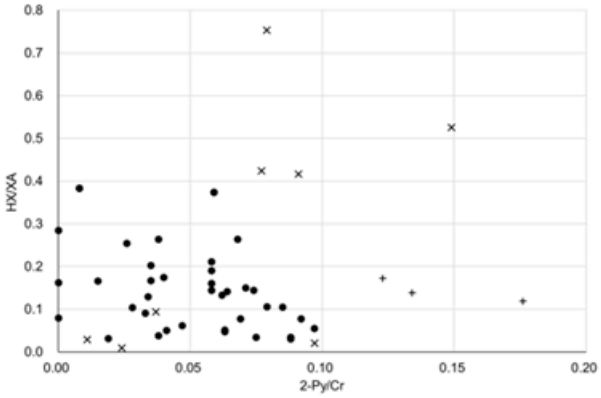


Figure 1C. Scatter plot of urinary 2-Py/Cr vs. urinary hypoxanthine/xanthine ratios of 48 *Xdh*KO mice
The three data points represented by pluses are excluded as outliers from the Figure 1A. Eight data points represented by crosses are also excluded as outliers from the Figure 1B.

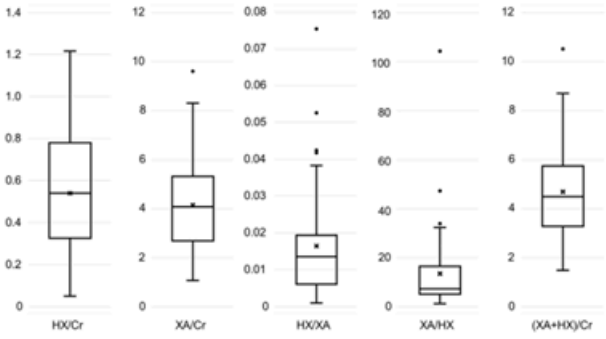


Figure 1B. Box and whisker plot of oxypurines in the urine of 48 *Xdh*KO mice.
The line and cross in the box represent the inclusive median and the average value, respectively. The outliers are repeesented by closed circles. Because an outlier of XA/Cr and (XA+HX)/Cr is from the same mouse, four outliers of HX/XA and three outliers of XA/HX constitute eight outliers.

Figure 1

Determination of outliers

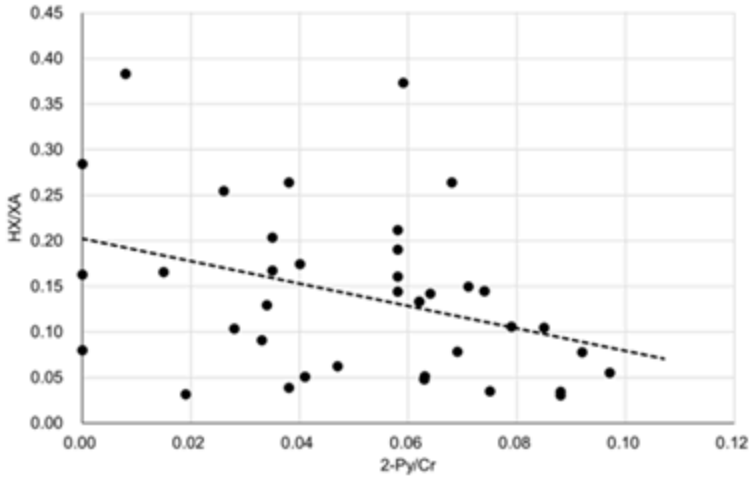


Figure 2A. Scatter plot of urinary 2-Py/Cr vs. urinary hypoxanthine/xanthine ratios of 37 *Xdh*KO mice after exclusion of outliers. The dotted line repecsents the regression line ($y = -1.23315x + 0.202485$, $r^2 = 0.130921$, $p = 0.027768$).

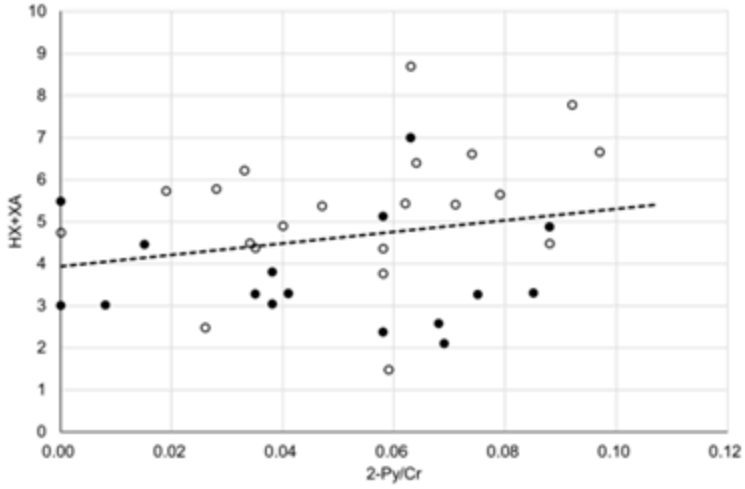


Figure 2B. Scatter plot of urinary 2-Py/Cr vs. urinary (xanthine + hypoxanthine)/Cr ratios of 37 *Xdh*KO mice after exclusion of outliers. The dotted line represents the regression line ($y = 13.70857x + 3.928103$, $r^2 = 0.049829$, $p = 0.184161$). Closed circles represent Slc23a4(-/-) mice. Open circles represent Slc23a4(+/) mice.

Figure 2

Urinary oxypurine profile of 37 *Xdh*KO mice

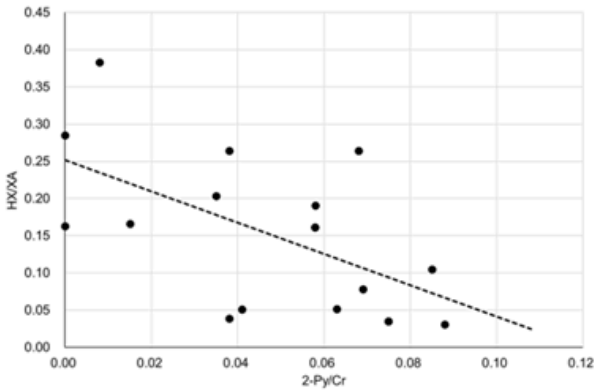


Figure 3A. Scatter plot of urinary 2-Py/Cr vs. urinary hypoxanthine/xanthine ratios of 17 *Xdh-Slc23a4* double KO mice. The dotted line represents the regression line (y = -2.1032x + 0.251614, r^2 = 0.329304, p = 0.020105).

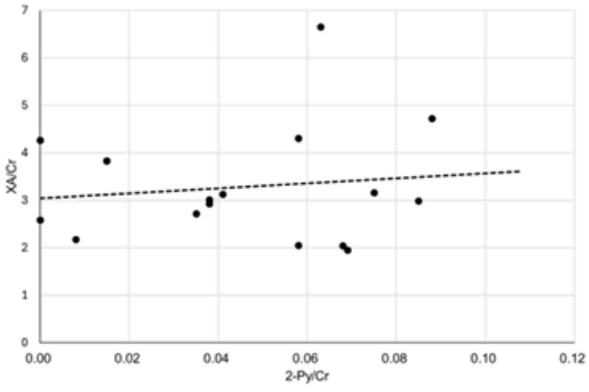


Figure 3D. Scatter plot of urinary 2-Py/Cr vs. urinary xanthine/Cr ratios of 17 *Xdh-Slc23a4* double KO mice. The dotted line represents the regression line. (y = 5.231622x + 3.044114, r^2 = 0.01508, p = 0.650496)

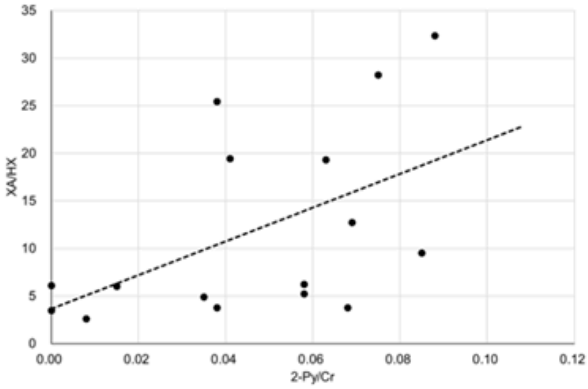


Figure 3B. Scatter plot of urinary 2-Py/Cr vs. urinary xanthine/hypoxanthine ratios of 17 *Xdh-Slc23a4* double KO mice. The dotted line represents the regression line. (y = 177.6625x + 3.632371, r^2 = 0.270974, p = 0.038707)

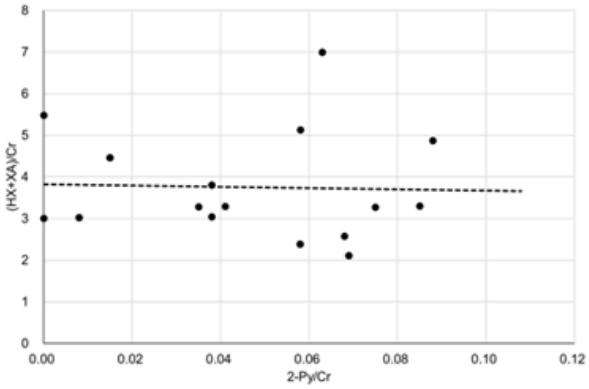


Figure 3E. Scatter plot of urinary 2-Py/Cr vs. urinary (hypoxanthine + xanthine)/Cr ratios of 17 *Xdh-Slc23a4* double KO mice. The dotted line represents the regression line. (y = -1.56183x + 3.826574, r^2 = 0.001203, p = 0.898548)

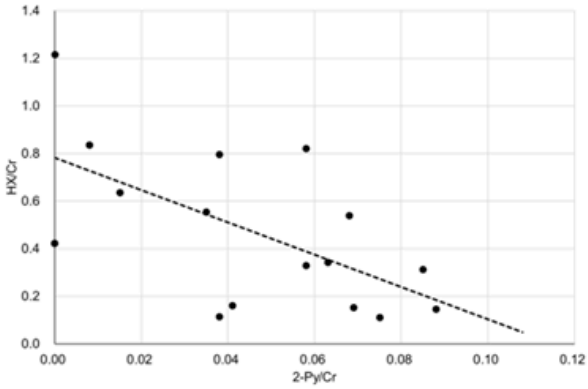


Figure 3C. Scatter plot of urinary 2-Py/Cr vs. urinary hypoxanthine/Cr ratios of 17 *Xdh-Slc23a4* double KO mice. The dotted line represents the regression line. (y = -6.79345x + 0.78426, r^2 = 0.369211, p = 0.012535)

Figure 3

Urinary oxypurine profile of 16 *Xdh*KO-*Slc23a4*KO mice

Supplementary Files

This is a list of supplementary files associated with this preprint. Click to download.

- SupplementaryInformation.docx